Reflectance properties of selected arctic-boreal land cover types: field measurements and their application in remote sensing

J. I. Peltoniemi, J. Suomalainen, E. Puttonen, J. Näränen, M. Rautiainen

Biogeosciences Discuss., 5, 1069–1095, 2008
www.biogeosciences-discuss.net/5/1069/2008/

Biogeosciences Discussions

Biogeosciences Discussions is the access reviewed discussion forum of *Biogeosciences*

Reflectance properties of selected arctic-boreal land cover types: field measurements and their application in remote sensing

J. I. Peltoniemi[1], **J. Suomalainen**[1], **E. Puttonen**[1], **J. Näränen**[2], and **M. Rautiainen**[3,4]

[1]Finnish Geodetic Institute, FI 02431 Masala, Finland
[2]Observatory, University of Helsinki, FI 00014 Helsinki, Finland
[3]Tartu Observatory, 61602 Tõravere, Estonia
[4]Department of Forest Ecology, University of Helsinki, FI 00014 Helsinki, Finland

Received: 3 January 2008 – Accepted: 18 January 2008 – Published: 5 March 2008

Correspondence to: J. I. Peltoniemi (jouni.peltoniemi@fgi.fi)

Published by Copernicus Publications on behalf of the European Geosciences Union.

Abstract

We developed a mobile remote sensing measurement facility for spectral and anisotropic reflectance measurements. We measured reflection properties (BRF) of over 100 samples from most common land cover types in boreal and subarctic regions. This extensive data set serves as a unique reference opportunity for developing interpretation algorithms for remotely sensed materials as well as for modelling climatic effects in the boreal and subarctic zones.

Our goniometric measurements show that the reflectances of the most common land cover types in the boreal and subarctic region can differ from each other by a factor of 100. Some types are strong forward scatterers, some backward scatterers, some reflect specularly, some have strong colours, some are bright in visual, some in infrared. We noted that spatial variations in reflectance, even among the same type of vegetation, can be well over 20%, diurnal variations of the same order and seasonal variation often over a factor of 10. This has significant consequences on the interpretation of satellite and airborne images and on the development of radiation regime models in both optical remote sensing and climate change research.

We propose that the accuracy of optical remote sensing can be improved by an order of magnitude, if better physical reflectance models can be introduced. Further improvements can be reached by more optimised design of sensors and orbits/flight lines, by the effective combining of several data sources and better processing of atmospheric effects. We conclude that more extensive and systematic laboratory experiments and field measurements are needed, with more modelling effort.

1 Introduction

The starting point for all scientific analysis of observational data is understanding its origin. In empirical sciences this understanding is reached by carrying out systematic experiments and by developing verified theories and models. Remote sensing is a

couple of crucial steps behind this.

The reflectance properties of land surfaces are of crucial importance in quantitative remote sensing and climate modelling. Today, the Earth is observed by thousands of airborne cameras and dozens of satellites. The number of observations will increase massively with the introduction of new, advanced fixed and mobile sensors, especially unmanned flying observation systems. Reflection models are also needed, e.g. in many industrial and security measurements, the development of intelligent sensors for autonomous vehicles, and visualisation projects.

A very complicated problem for the more accurate analysis of the data is the significant anisotropy of the target reflectance: the brightness and colour (spectrum) of the target depend heavily on the direction in which the target is illuminated, and on the direction in which it is observed. This dependence on the two directions is described using a *bidirectional reflectance distribution function* (BRDF) or *bidirectional reflectance factor* (BRF), which gives the ratio of the radiation reflected by the target to radiation reflected by the ideal white isotropic (Lambertian) reflector (see Fig. 1 for the definition of measurement geometry and angles). The unfortunate thing is that the BRF of each target is different and in most cases rather unknown. Thus, even just comparing two images taken in a different illumination or observation direction (or even opposite sides of one image!) is complicated, not to mention any attempt to make more use of quantitative brightness and spectral data. Of course, the varying bidirectional effect also promises new attractive opportunities for target characterisation. Many instruments already provide useful multidirectional data (MISR Diner et al., 2005, CHRIS/PROBA Guanter et al.; Barnsley et al.; Barnsley et al., 2005; 2000; 2004) POLDER Hautecoeur and Leroy; Bicheron and Leroy, 1998; 2000, HRSC Neukum (2001); Kukko et al. (2005). The new digital photogrammetric airborne cameras – DMC, ADS 40, Ultracam D/X, etc. – can, when properly calibrated, provide excellent directional radiometric data in very high spatial resolution (Markelin et al., 2008; Honkavaara, 2008).

Numerous attempts have been made to model the BRDF. The RAMI benchmark (Widlowski et al., 2006) contains 18 models for vegetation, and there is still extensive

work to be carried out on forests (Rautiainen, 2005; Rautiainen et al., 2007; Smolander, 2006), fields, soil (Cierniewski et al., 2004; Mishchenko et al., 1999; Stankevich and Shkuratov, 2004), snow (Peltoniemi, 2007), and waters. Despite clear success, the current models still have several problems: most are rather weakly validated, many are developed for a specific instrument only or to a limited wavelength range, and often contain unphysical parameters.

Climate models require the land surface albedo to be known at a quite high absolute accuracy, from 0.02 to 0.05 (Jin et al., 2003). Several instruments provide global and local albedos, e.g. MODIS at Terra and Aqua (Liang et al., 2005; Wang et al., 2007). The methology is mostly based on a parametrised BRF (e.g. RossThick-LiSparse), applied to near nadir observation (Liang et al., 2005). MISR can provide multidirectional observations, but with less coverage (Diner et al., 2005). Locally, albedos are often measured using mast–based or portable albedometers, and airborne measurements. It still remains somewhat unclear how accurately these instruments can measure albedos of real, very heterogeneous nature, how long the data remain valid and how many model dependencies there are.

Constant experimental research must be carried out on remote sensing and climate sciences, on all scales. One class of instruments that measure the detailed reflection properties of targets is field/laboratory goniospectrometers. These measure the accurate directional and spectral dependence of the scattered light. In remote sensing applications, the most used instruments measure a footprint of about 10 to 30 cm in diameter (Hosgood et al., 2000; Sandmeier and Itten, 1999; Turner, 1998; Painter et al., 2003; Peltoniemi et al., 2005b,a). An alternative way is to measure all directions from one point, e.g. a mast, which will yield the BRF, if the target is homogeneous over a full observational range. A small database of BRF data from vegetation is given by von Schönermark et al. (2004), and another one is evolving at the University of Zürich (Hüni et al., 2007)

In this paper, we describe a recent, significant advance in goniometric reflectance measurement techniques which has been used for collecting an extensive data set

covering typical land cover types in the boreal and subarctic regions. We present results from the new data bank, quantitatively evaluate differences in the BRFs of the land cover types and, finally, discuss measures needed for the improvement of the current optical remote sensing scene.

2 Instruments and measurements

The new measurements taken using the Finnish Geodetic Institute Field goniospectrometer 6 (Figifigo), see Fig. 2. Our database also includes measurements taken using older instruments, especially our previous goniometer model 3 (Peltoniemi et al., 2005b,a) and European Goniometer Facility (EGO) (Peltoniemi et al., 2007).

The Figifigo system consists of a motor-driven moving arm, tilting ±90° from the vertical, variable fore optics in the high end of the arm, and an ASD Field Spec Pro FR 350–2500 nm spectrometer. Accurate angles are read by using an inclinometer and an electronic compass. The position is given by using GPS. The system can be mounted on a light sledge for snow measurement, on a rotating ring for laboratory measurement or manually moved and rotated by two persons. Recently, a calcite Glan–Thomson prism has been installed to measure polarisation at full wavelength range (Polarisation measurements will be reported in another research article). Typically, the footprint diameter is about 10 cm (3 to 30 cm possible), elongating at larger sensor zenith angles as $1/\cos\theta$, and wandering around a few cm by bending and azimuthal movements.

Measurements were mostly taken outside in the fields, under direct sunlight. The instrument was calibrated using a Labsphere Spectralon 99% white reference plate before and after each turn. The reflection spectra at available angles were measured by swinging the sensor arm and turning the instrument around the target, starting (and ending) with the principal plane. The diffuse skylight was measured separately and optionally subtracted from the measurement data to obtain the most accurate BRF. Sunlight was monitored continuously by a pyranometer. Measurement of one hemisphere at one illumination angle took between 10 and 60 min, depending on the sky

condition and various technical aspects. The spatial variations of some samples were analysed more carefully by taking large sets of additional spectra with a nadir view (looking straight down) and walking with the instrument over the selected area.

Some samples were measured in the darkness of night or inside using using an Oriel 1000 W quartz tungsten halogen (QTH) research light source. This allowed for the systematic variation of illumination angles, but the imperfect light distribution caused possible unrecoverable systematic errors of up to 10%.

The targets were carefully selected to be relatively pure and to have a visually homogeneous area with a diameter of about 30 cm. It was occassionally necessary to clean away debris and other disturbing vegetation. The sampling is thus not most representative of the typical natural surroundings, but of more ideal targets. Typical samples are strongly heterogeneous in many parameters and in many scales even inside the observation spot, which makes interpreting the results complicated. For documentation and analysis, the targets were photographed and many measurable properties were measured.

Data were checked, cleaned, and stored in a database. Depending on the case, the measured intensity from target (I) was normalised by measured intensity from reference target (I_{STD}), a diffuse background (I_{DIFF}) was subtracted and the reference target refractivity (R_{STD}) applied

$$R(\mu, \mu_0, \phi, \phi_0) = \frac{I - I_{\mathrm{DIFF}}}{I_{\mathrm{STD}} - I_{\mathrm{SDIFF}}} R_{\mathrm{STD}}(\mu, \mu_0, \phi, \phi_0). \quad (1)$$

To compose a coherent averaged presentation of several measurements of slightly varying samples and continuously moving sun, one of the parametric functions below was fitted to the data

$$R(\mu,\mu_0,\alpha,\gamma) = \frac{1}{\mu+\mu_0} \times \mathrm{e}^{\sum_{ji}^{N}\left(a_i^j P_i(\alpha)+b_i^j P_i(\beta)\mathrm{e}^{-\frac{\beta^2}{2}}+c_i^j P_i(\delta)\mathrm{e}^{-\frac{\delta^2}{2}}\right)S^j(\mu,\mu_0)}, \quad (2)$$

$$R(\mu,\mu_0,\alpha,\gamma) = \frac{1}{\mu+\mu_0}\sum_{ji}^{N} S^j(\mu,\mu_0) \times \left(a_i^j P_i(\alpha) + b_i^j P_i(\beta)\mathrm{e}^{-\frac{\beta^2}{2}} + c_i^j P_i(\delta)\mathrm{e}^{-\frac{\delta^2}{2}}\right), \quad (3)$$

where a, b, c are wavelength dependent expansion coefficients, $\beta = \tan(\alpha/2)/\tan(5^\circ/2)$, $\delta = \tan(\gamma/2)/\tan(5^\circ/2)$, γ is the specular phase angle, defined as $\cos\gamma = (\mu + \mu_0)/\sqrt{2+2\cos\alpha}$, P_i is a polynominal, and $S(\mu,\mu_0) = [1, \mu+\mu_0, \mu\mu_0, \mu^2+\mu_0^2]$. This expansion assumes explicit reciprocity, left–right symmetry, isotropy in the solar azimuth ($R(\phi,\phi_0) = R(|\phi - \phi_0|)$, and certain smoothness of BRF shape-much stronger than the measurement data provide. The actual order of the expansion depends on the shape of the BRF, the number and distribution of data points, and whether one wants a smooth presentation of a single data set or wide interpolation and extrapolation to large angular range. In general, the phase angle dependence is by far the most important, and it is seldom needed to take even the second order in μ. The exponential form (Eq. 2) is preferred over the linear (Eq. 3) when it is important to get good relative accuracy for both large and small values and keep the values always positive. On the other hand the linear form (Eq. 3) gives better absolute accuracy and a little bit safer extrapolation. The albedo is estimated by integrating numerically the linear expansion. This expansion is here used only as a presentation and averaging tool, and for more detailed analysis more physical models are of course needed.

3 Results

A summary of the most important measurement campaigns and samples is presented in Table 1 and locations in Fig. 3. A selected set of results from several representative land cover types combined from all the suitable measurements is shown in Figs. 4–4. First, an illustrating photograph is shown by one actually measured sample. The averaged reflectance spectra are plotted from three observation directions and a single illumination direction. The darker colour gives the standard deviation of sample reflectances in the nadir view, and the lighter colour the max/min values, illustrating the sample inhomogeneities. Two 3D BRF diagrams show the anisotropy pattern, integrated over the red (here using the DMC sensitivity) and near infrared (ADS NIR channel) parts of the spectrum (snow over the MERIS/MISR/POLDER/etc blue 443 nm and MODIS 6: 1628–1652 nm to give better contrast). For easier comparison, the plots are interpolated to the solar zenith angle of about 50°, or closest useful: snow and dwarf birch 58°, cotton grass 62°.

For a few samples also albedo plots are shown, to point out some subtle differences in spectra (Fig. 4).

The scattering anisotropy is significant in all the measured samples; we have not seen any even closely isotropic targets in natural surroundings. The anisotropy effect is always much bigger at large solar zenith angles than smaller zenith angles. The variation is always strongest at the principal plane, and usually weakest close to the cross plane (90 degrees from the principal plane). The directional properties of the targets vary over a very large range, depending on the not yet completely understood physical (density, orientation, size) and chemical (composition, wetness) properties of the targets, but some support for target identification and structural inversion is given. Different spectral bands have usually somewhat differing anisotropy, although usually the differences are not dramatic. Most typically bright bands are more isotropic than dark bands; the multiply scattered light is always more isotropic than singly scattered, although the single (and sometimes double and third order) anisotropy always remains.

All samples but snow show strong back scattering (hot spot) effect. Many targets have also clear forward brightening. The presence of liquid water adds to specular angle effect. The so called dark spot can be located in roughly half of the samples, but its location varies in large range from about nadir to wide forward.

The strongest signature between various targets is still the spectrum. The spectral shape depends on the view and illumination angles, absolutely and relatively, but most significant features behave rather consistently. In some cases the specular and forward parts show some additional colour effect compared with other directions, and some two layer media show clear differences between nadir and large zenith angle view. Almost all the presented targets can be well identified from all directions, but quantitative analysis requires a well-known BRF.

Below, we discuss some measured sample categories in more detail.

Pure sand (Fig. 4, top) can form quite homogenenous areas at beaches and in deserts. Typically, sand has strong back scattering and varying forward scattering enhancement. The spectral shape is known to show large variations, but all our samples are quite similar, even though taken from 4 places in Finland that are very far apart (from Hanko to Sodankylä, Fig. 3).

Organic soil (Fig. 4, 2. row) varies a great deal, depending on its content. Typically, it has rather strong backscattering, but some types have a forward scattering feature, too. The spectrum can be quite flat, or brighten towards the NIR, depending on the organic content, but it appears to be well between sand and peat values. Wetness can change spectral and directional features significantly. There is often a significant amount of debris and droppings.

Snow (Fig. 4, 3. row) is the brightest of natural targets in visual wavelengths, but darkens rapidly when the wavelength increases above 900 nm. The grain size, shape, and surface topography effect the spectrum and anisotropy. Forward scattering is strong in all wavelengths and snow types. Snow will be discussed in much more detail in following publications.

Peat (Fig. 4, top) is also a backscatterer. The spectrum is brownish, increasing from

400 nm to 1300 nm. Wetness darkens reflection spectrum clearly in all wavelengths (Fig. 4).

Moss (mostly *Hylocomium splendens*, with some *Pleurozium schreberi*, *Dicranum polysetum*, Fig. 4, 2. row) also shows large variations. Some types are strong forward scatterers, some backward scatterers, and some in between. A yellowish spectrum separates most moss from other typical understorey.

Lichen (mostly *Cladina arbuscula* and *C. rangiferina*, Fig. 4, 3. row) is very identifiable by a clearly brighter reflectance in all visual bands than green vegetation. All measured lichen are more or less strong backscatterers – actually among the strongest we have measured. Lichen abundances should thus be rather invertible from spectral-directional data.

Cotton grass (*Eriophorum vaginatum*, Fig. 4, 4. row) is brighter than most vegetation in all wavelengths. The white tassel gives clear signature.

Grass (Fig. 4, bottom) (including natural, garden and football pitches), shows the "purest" green vegetation spectrum of all the measured samples, i.e. sharpest green spike at 550 nm and brightest at near infrared 800–1300 nm. It has some backward enhancement, but it is weaker compared with most other samples.

Dwarf shrubs (Fig. 4) have many common features: all have some backward enhancement and bowl shapeness.

Blueberry (*Vaccinium myrtillus*) and lingonberry (*Vaccinium vitis-idaea*) with their wax leaves have additionally clear forward brightening, which means they can be easily distinguished from e.g. heather (*Calluna vulgaris*), which is the strongest backscatterer of the measured shrubs. Crowberry (*Empetrum nigrum*) is also more of a backscatterer. Dwarf birch (*Betula nana*) is between lingonberry and crowberry.

4 Conclusions and discussions

We have measured the spectral BRF of over 100 samples of typical boreal and subarctic land cover types using our mobile field goniospectrometers. We have observed

that these target types have greatly differing reflection properties. Anisotropy can vary by a factor of 10, spectral properties by a factor of 100. Even the reflectances of the same type of targets vary spatially and temporarily by a factor of at least 10% to 50%, depending on their state and condition. The reflectance spectrum (colour) depends clearly on directions, both absolutely and relatively, but the strongest and most typical signatures are usually seen in all directions. Extracting quantitative information accurately, even as simple as vegetation indices, from spectral data requires the BRF to be well known. Only indices and comparisons based on bands of about equal brightness could be direction invariant in favourable conditions.

The averaged, fitted and smoothed presentation is not giving the full picture of BRF properties. Individual samples provide richer structure, often with several maxima and minima, clear left–right asymmetry, solar azimuth dependence, and local irreciprocity (not braking any laws for small samples with 3-D structure).

The inversion of the spectral-directional data to retrieve information on the structural and chemical properties of the targets provokes many challenges which, until now, have not received sufficient attention. A major difficulty is the enormous variability and heterogeneity of nature, in all scales, continuous and stepwise, causing very large effects on reflectances (see Fig. 4). Basically all modelling, measurements, and validations are done with idealised, carefully selected and prepared samples (most homogeneous, isotropic, stable, flat). Thus the applicability of all remote sensing techniques to true nature is still in question. Solving all this requires hierarchical bio/geo/physical models, i.e. the parameters and predictions must be measurable physical quantities. This parameter base shall be strongly constrained by biological/ecological/geophysical/geological/geographical conditions, and the modelling should start from the smallest units (leave, needle, dust grain; even internals down to molecule scale) building larger and larger blocks (shoots, branches, trees, overstorey vegetation, soil, understorey, forest, . . .). The models should also try to aim to apply to multiple observations types – active and passive; optical, thermal, microwave; spectral, directional, polarised, imaging, etc. – instead of a separate model for each instrument

set-up. This would allow easier and more flexible use of different instrument palettes in varying conditions.

The atmosphere frequently disturbs the measurements. Although in a few dry and clear periods its properties can stay quite stable for days, more often there are all kinds of variations over all time and length scales. In particular the water vapour abundance varies, making any spectral bands near water vapour absorption bands unreliable. Thin, almost invisible cirrus causes variations of about 10% quite often, and larger clouds cause not only shadowing, but a significant amount of diffuse radiation that affects the target brightness by 10 to 20%. Aerosol contribution is still weakly characterised, but often significantly disturbing. Monitoring the sun and sky continuously and simultaneously during the measurement is thus absolutely necessary for all observations, not only on the ground, but for airborne sensing, too, if physical and invertible data is wanted.

From the analysed data we recommend for passive optical sensors the following

1. nothing can beat high spatial resolution when observing broken, heterogeneous, rough, and multi-scale terrains. Even a monochromatic image allows sectioning and identification by brightness, shapes and textures, which will significantly promote further analysis, and give a starting point for more detailed model inversion.

2. a few waveband channels can already improve target identification in a great extent, and high resolution spectrometry yields much more recoverable information, up to quantitative composition analysis. Hyperspectral imaging sensors are thus highly recommended.

3. hyperspectrometry should always be accompanied by multidirectional observations, to compensate for the anisotropy effects and support structural inversion. At least 7–11 directions near the principal plane and a few directions in cross directions, with a sufficiently wide range ±60° to ±70°, should be observed. At the beginning, multidirectional observations can well be taken at lower spectral resolution than primary spectrometry, because the spectral-directional effects are

still rarely too surprising. At a later stage one can also increase full spectral directions, although it is still probably more optimal to do most directional observing at a lower spectral resolution.

4. the useful dynamic range of cameras and sensors should be at least 100, with an accuracy of 1%, when heterogeneous land is observed, even more, if the image contains especially dark objects (e.g. shadows) or bright ones (snow in forward, specular surfaces, sunfacing slopes etc.). At least 12 bit data storage is needed.

5. appropriate solar and atmospheric sensors must be integrated on all airborne systems to be able to produce quantitative, atmosphere-compensated observation data in varying conditions.

The flight line (or satellite orbit) must be planned directly towards or away from the sun (±10°), in order to obtain the most invertible anisotropy data in forward-backward directions (near the principal plane) and minimal anisotropy in side directions. For the most accurate analysis, the sensors should also be calibrated using well-known on-ground reference targets during the flight, but this is, of course, impractical for large area observations. None of the measured targets applies as an ad hoc reference without check, because their properties vary. Pure new snow or dry sand could be closest, if one can fix the key parameters.

For albedo mapping these results indicate that the uncertainties may be larger than studies made in carefully selected ideal sites claim (Salomon et al., 2006; Jin et al., 2003; Baret et al., 2005). Reliable albedo measurements from heterogeneous surfaces are very challenging even on the ground. Typical albedometers have fields of view from some 50° to 80°, missing the brightest forward and backward scatterings, which itself can cause errors of 5% to 20%, depending on the scattering properties of the target and instrument bias (Peltoniemi, 2007), especially at low solar illumination, which is usual in boreal and subarctic latitudes. More errors will certainly occur if the albedo has to be estimated from one observation direction assuming some parametric BRF shape. The typical heterogeneity of boreal land reflectivity can be well over 100% even

during the summer, and a factor of 10 during the winter. Diurnal variations also seem to be around 5% to 20% (Pirazzini, 2004; Flanner and Zender, 2006, also e.g.), and seasonal certainly more.

We have demonstrated that even simple, lightweight instruments can yield large amounts of valuable data, but simplicity has its limits. New facilities are urgently needed for measuring both larger and smaller scales (<mm to >10 m), measuring more complete diurnal and seasonal time series, for combining active and passive optical, thermal, and microwave experiments together, and for simulating various observation concepts in true and miniature scales.

Actually, the whole remote sensing development chain would benefit from complete restructuring, starting with thorough empirical and theoretical basic research, leading to new sensor prototypes and observation concepts to be tested in laboratory and field conditions and computer simulations, maturing systems in airborne operations, and finally with that experience building superior satellite systems.

Currently, we are extending the data bank to include new samples from different geographical locations. In addition, we are studying polarisation effects which are proving to be a significant source of information on the properties of common terrestrial cover types. The technical development of the goniometric instruments, especially their mobility and the level of automation, and the possibility of using them in small UAV-based goniospectrometry measurements are also central issues in our research. We believe that, in the future, more emphasis needs to be placed on basic in situ reflectance measurements and the thorough quantification of anisotropy patterns of land cover types. This will significantly benefit both the remote sensing and climate change research communities.

Acknowledgements. Goniometers 2 and 3 were built at Helsinki University of Technology, Goniometer 5 at Helsinki Polytechnics Stadia. Measurement campaigns have been funded by EU projects Norsen, Omega and Enamors, by the Ministry of Agriculture and Forestry, Academy of Finland. M. Hirschmugl, J. Torppa, H. Smolander, S. Smolander, P. Stenberg, M. Mõttus, P. Voipio, L. Markelin, F. Bergholm, H. Tömmervik, E. Kyrö, J. Piironen, B. Hosgood, B. Clark, P. Pellikka, S. Kaasalainen, L. Matikainen, T. Hakala, R. Kuittinen, J. Hyyppä, and many others

have assisted with measurements, campaign design and data. Author Contributions: JP collected the paper and supervised the research, JS has developed the goniometers and made most of the measurements since 2004, JN before that, MR contributed to interpretation of results and forest understanding, and all authors contributed to the writing.

References

Baret, F., Schaaf, C., Morisette, J., and Privette, J.: Report on the Second International Workshop on Albedo Product Validation, Earth Observer, 2005.

Barnsley, M., Lewis, P., O'Dwyer, S., Disney, M., Hobson, P., Cutter, M., and Lobb, D.: On the Potential of CHRIS/PROBA for Estimating Vegetation Canopy Properties from Space, Remote Sensing Reviews, special Issue on the 2nd International Workshop on Multi-angular Measure- ment and Modelling (IWMMM-2), 2000.

Barnsley, M., Settle, J., Cutter, M., Lobb, D., and Teston, F.: The PROBA/CHRIS mission: a low-cost smallsat for hyperspectral multiangle observations of the Earth surface and atmosphere, IEEE Transactions on Geoscience and Remote Sensing, 42, 1512–1520, 2004.

Bicheron, P. and Leroy, M.: Bidirectional reflectance distribution function signatures of major biomes observed from space, J. Geophys. Res., 105, 26 669–26 681, 2000.

Cierniewski, J., Gdala, T., and Karnieli, A.: A hemispherical-directional reflectance model as a tool for understanding image distinctions between cultivated and uncultivated bare surfaces, Remote Sensing of Environment, 90, 505–523, 2004.

Diner, D. J., Braswell, B., Davies, R., Gobron, N., Hu, J., Jin, Y., Kahn, R., Knyazikhin, Y., Loeb, N., Muller, J.-P., Nolin, A., Pinty, B., Schaaf, C., Seiz, G., and Stroeve, J.: The value of multiangle measurements for retrieving structurally and radiatively consistent properties of clouds, aerosols, and surfaces, Remote Sensing of Environment, 97, 495–518, 2005.

Flanner, M. G. and Zender, C. S.: Linking snowpack microphysics and albedo evolution, J. Geophys. Res., 111, D12208, doi:10.1029/2005JD006834, 2006.

Guanter, L., Alono, L., and Moreno, J.: First Results from the PROBA/CHRIS Hyperspectral/Multiangular Satellite System Over Land and Water Targets, IEEE Geoscience and Remote Sensing Letters, 2, 2005.

Hautecoeur, O. and Leroy, M.: Surface bidirectional reflectance distribution function observed at blobal scale by POLDER/ADEOS, Geophys. Res. Lett., 25, 4197–4200, 1998.

Honkavaara, E.: Calibrating digital photogrammetric airborne imaging systems using test field, Ph.D. thesis, Helsinki University of Technology, 2008.
Hosgood, B., Sandmeier, S., Piironen, J., Andreoli, G., and Koechler, C.: Goniometers, in: Encyclopedia of Electronics Engineering, edited by Webster, J., 8, 424–433, John Wiley, New York, 2000.
Hüni, A., Nieke, J., Schopfer, J., Kneubähler, M., and Itten, K.: Metadata of Spectral Data Collections, 5th EARSeL Workshop on Imaging Spectroscopy, Bruges, Belgium, 2007.
Jin, Y., Schaaf, C. B., Woodcock, C. E., Gao, F., Li, X., Strahler, A. H., Lucht, W., and Liang, S.: Consistency of MODIS surface bidirectional reflectance distribution function and albedo retrievals: 2. Validation, J. Geophys. Res., 108, 4159, doi:10.1029/2002JD002804, 2003.
Kukko, A., Hyyppä, J., and Kuittinen, R.: Use of HRSC-A for sampling bidirectional reflectance, ISPRS Journal of Photogrammetry and Remote Sensing, 59, 323–341, 2005.
Liang, X.-Z., Xu, M., Gao, W., Kunkel, K., Slusser, J., Dai, Y., Min, Q., Houser, P. R., Rodell, M., Schaaf, C. B., and Gao, F.: Development of land surface albedo parameterization based on Moderate Resolution Imaging Spectroradiometer (MODIS) data, J. Geophys. Res., 110, D11107, doi:10.1029/2004JD005579, 2005.
Markelin, L., Ahokas, E., Honkavaara, E., Peltoniemi, J., Kukko, A., Hyyppä, J., and Kuittinen, R.: Portable reflectance targets and their use in radiometric evaluation and calibration of digital photogrammetric cameras, Photogrammetric Engineering and Remote Sensing, in press, 2008.
Mishchenko, M. I., Dlugach, J. M., Yanovitskij, E. G., and Zakharova, N. T.: Bidirectional reflectance of flat, optically thick particulate layers: an efficient radiative transfer solution and applications to snow and soil surfaces, J. Quant. Spectrosc. Radiat. Transfer, 63, 409–432, 1999.
Neukum, G.: The airborne HRSC-AX cameras: evaluation of the technical consept and presentation of application results after one year of operations, in: Photogrammetric Week 2001, edited by Fritsch/Spiller, 117–130, 2001.
Painter, T. H., Paden, B., and Dozier, J.: Automated spectro-goniometer: A spherical robot for the field measurement of the directional reflectance of snow, Review of Scientific Instruments, 74, 5179–5188, 2003.
Peltoniemi, J., Kaasalainen, S., Näränen, J., Matikainen, L., and Piironen, J.: Measurement of directional and spectral signatures of light reflectance by snow, IEEE Transactions on Geoscience and Remote Sensing, 43, 2294–2304, 2005a.

Peltoniemi, J., Kaasalainen, S., Näränen, J., Rautiainen, M., Stenberg, P., Smolander, H., Smolander, S., and Voipio, P.: BRDF measurement of understory vegetation in pine forests: dwarf shrubs, lichen and moss, Remote Sensing of Environment, 94, 343–354, 2005b.

Peltoniemi, J., Piironen, J., Näränen, J., Suomalainen, J., Kuittinen, R., Honkavaara, E., and Markelin, L.: Bidirectional reflectance spectrometry of gravel at the Sjökulla test field, ISPRS Journal of Photogrammetry and Remote Sensing, 62, 434–446, 2007.

Peltoniemi, J. I.: Spectropolarised ray-tracing simulations in densely packed particulate medium, J. Quant. Spectrosc. Radiat. Transfer, 108, 180–196, http://dx.doi.org/10.1016/j.jqsrt.2007.05.009, 2007.

Pirazzini, R.: Surface albedo measurements over Antarctic sites in summer, J. Geophys. Res., 109, D20118, doi: 10.1029/2004JD004617, 2004.

Rautiainen, M.: The Spectral Signature of Coniferous Forests: the role of stand structure and leaf area index, Ph.D. thesis, University of Helsinki, Department of Forest Ecology, pubslihde in Dissertationes Forestales, Number 6, 2005.

Rautiainen, M., Suomalainen, J., Ml ottus, M., Stenberg, P., Voipio, P., Peltoniemi, J., and Manninen, T.: Coupling forest canopy and understory reflectance in the Arctic latitudes of Finland, Remote Sensing of Environment, 110, 332–343, 2007.

Salomon, J., Schaaf, C. B., Strahler, A. H., Gao, F., and Jin, Y.: Validation of the MODIS Bidirectional Reflectance Distribution Function and Albedo Retrievals Using Combined Observations from the Aqua and Terra Platforms, IEEE Transactions on Geoscience and Remote Sensing, 44, 2006.

Sandmeier, S. R. and Itten, K. I.: A Field Goniometer system (FIGOS) for acquisition of hyperspectral BRDF data, IEEE Transactions on Geosciences and Remote Sensing, 37, 648–658, 1999.

Smolander, S.: Radiative transfer, interception and scattering in coniferous forests: models and applications for production ecology and remote sensing, Ph.D. thesis, University of Helsinki, published in Dissertationes Forestales, Number 22, 2006.

Stankevich, D. and Shkuratov, Y.: Monte Carlo ray-tracing simulation of light scattering in particulate media with optically contrast structure, J. Quant. Spectrosc. Radiat. Transfer, 87, 289–296, 2004.

Turner, M.: The Sandmeier Field Goniometer: A measurement tool for bi–directional reflectance, in: NASA Commercial Remote Sensing Verification and Validation Symposium, 1–6, 1998.

von Schönermark, M., Geiger, B., and Räser, H.-P.: Reflection Properties of Vegetation and Soil With a BRDF-Data base, Wissenschaft und Technik, 2004.
Wang, Z., Zeng, X., and Barlage, M.: Moderate Resolution Imaging Spectroradiometer bidirectional reflectance distribution function-based albedo parameterization for weather and climate models, J. Geophys. Res., 112, D02103, doi:10.1029/2005JD006736, 2007.
Widlowski, J.-L., Taberner, M., Pinty, B., Bruniquel-Pinel, V., Disney, M., Fernandes, R., Gastellu-Etchegorry, J.-P., Gobron, N., Kuusk, A., Lavergne, T., Leblanc, S., Lewis, P., Martin, E., Mõttus, M., North, P. J. R., Qin, W., Robustelli, M., Rochdi, N., Ruiloba, R., Soler, C., Thompson, R., Verhoef, W., Verstraete, M. M., and Xie, D.: The third RAdiation transfer Model Intercomparison (RAMI) exercise: Documenting progress in canopy reflectance modelling, J. Geophys. Res., 112, D09111, doi:10.1029/2006JD007821, 2006.

Table 1. Most important measurement campaigns. Year, month, location (FI=Finland, SE=Sweden, NO=Norway, AU=Australia, AT=Austria), used instrument (G1=goniometer Model 1 with Photo Research PR 713, G2= Model 2 with PR-713, G3=goniometer model 3 with ASD Field Spec Pro FR, G4=model 4 with ASD, G 5=Model 5, F=Figifigo, FP=Figifigo with polariser, A=SD hand held, O=using Oriel 1000 W lamp, L5 using 500 W theater lamp, L3 using 300 W industrial halogen, otherwise using Sun, M=mast mounted spectrometer by FMI).

date	location	samples	instrument
1996 07	Sjökulla, FI	gravel	G1
1998 03	Vuotso, FI	snow	G2, L3
2001 02	Hyytiälä, FI	new snow	G3
2001 05	Sodankylä, FI	old snow	G3
2001	Masala, Metsähovi, FI	grass	G3
2002	Rovaniemi, FI	new snow	G3
2002–3	Masala, FI	branches of trees, leaves, grasses	G3
2002 09	Hintereisferner, AT	snow, ice, firn	G4,A
2003 08	Suonenjoki, FI	forest understorey	G3,A,L5
2004	Sodankylä, FI	snow	G3,O
2004	Sjökulla, FI	gravel	G3
2004	Metsähovi, FI	grass, moss, lichen	G3
2005 04	Sodankylä, FI	snow	G5,O
2005 08	Suonenjoki, FI	forest understorey	F,O
2005	Helsinki, Espoo, FI	parking slot, beach	F,A
2005	Masala, lab, FI	understorey	F,O
2006 03	Sydney, AU	grass	F
2006	Espoo, Masala, FI	asphalts	F
2006 08	Sodankylä, FI	forest understorey, soil, open land	F,M
2006 08	Andøya, NO		F
2006 08	Abisko, SE	lake water, mountain vegetation	F, boat mounted
2007 04	Sodankylä, FI	melting snow	FP
2007 07	Sodankylä, FI	forest understorey, open land	FP

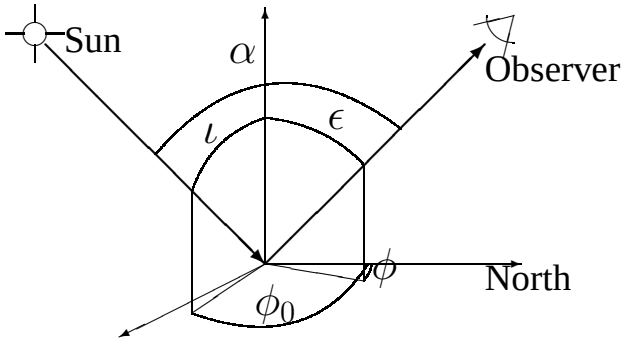

Fig. 1. Measurement geometry: ϵ and ι are the zenith angles of the emergent (observer) and incident (solar) radiation respectively. ϕ and ϕ_0 are the corresponding azimuths. The phase or back scattering angle α is the angle between the observer and the Sun. The principal plane is fixed by the solar direction and the surface normal, while the cross plane is a vertical plane perpendicular to the principal plane.

BGD
5, 1069–1095, 2008

Fig. 2. Figifigo measuring BRF in Abisko, Sweden.

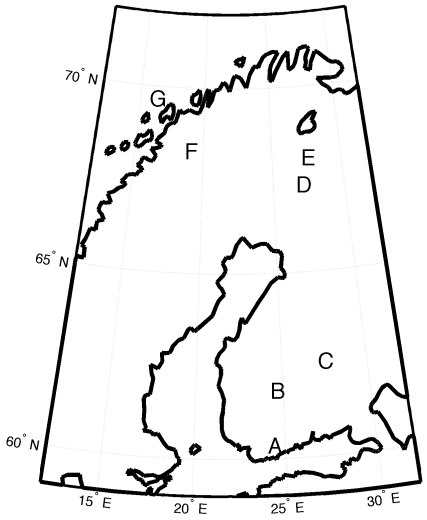

A) Espoo (60.21°N 24.66°E)
Metsähovi (60.22°N 24.39°E)
Masala (60.15°N 24.53°E)
B) Hyytiälä (61.84°N 24.29°E)
C) Suonenjoki (62.58°N 27.17°E)
D) Sodankylä (67.37° N 26.63°E)
E) Vuotso (68.09°N 27.12°E)
F) Abisko (68.31°N 18.65°E)
G) Andoya (69.18° N 16.08°E)

Fig. 3. The locations for the most important measurement campaigns. Not included on the map are Sydney (Australia) and Hintereisferner (Austria).

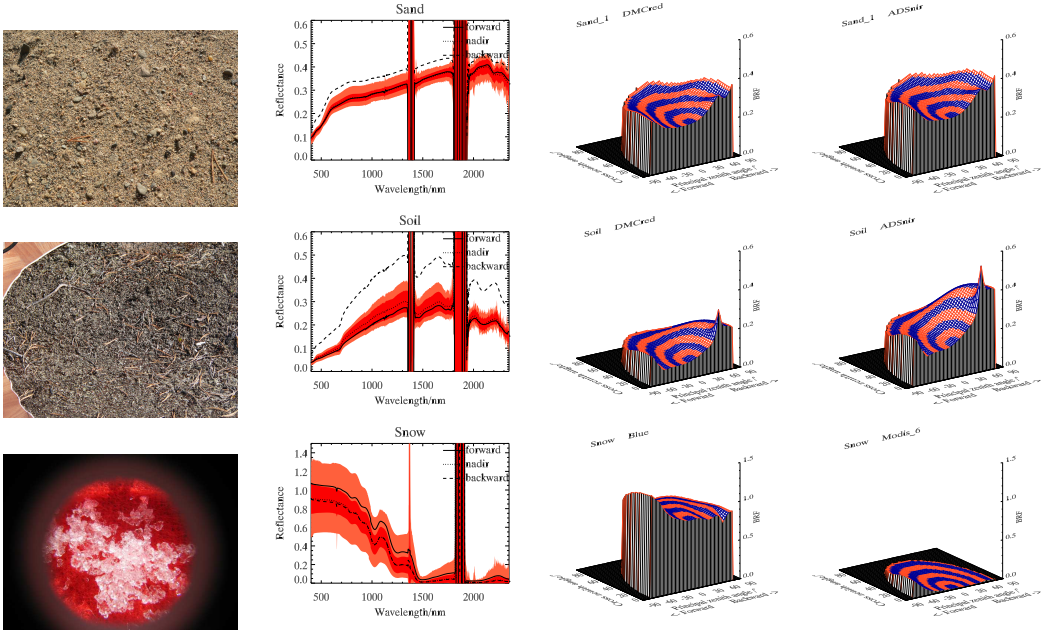

Fig. 4. Sample results of various targets. Leftmost a photo of the target, middle-left reflection spectra in three directions (solid line forward 50°, dotted line nadir, dashed line backward 50°), with sample inhomogeneity shown as grey levels, darker gray standard deviation and lighter grey max/min values from nadir view, middle-right BRF diagram in red and rightmost in near infrared 800–900 nm band. Plots are shown at 50° angle of incidence, unless otherwise given. The targets are, top down: sand, soil, snow (bands: blue and NIR 1200–1300 nm, angle of incidence: 58°.

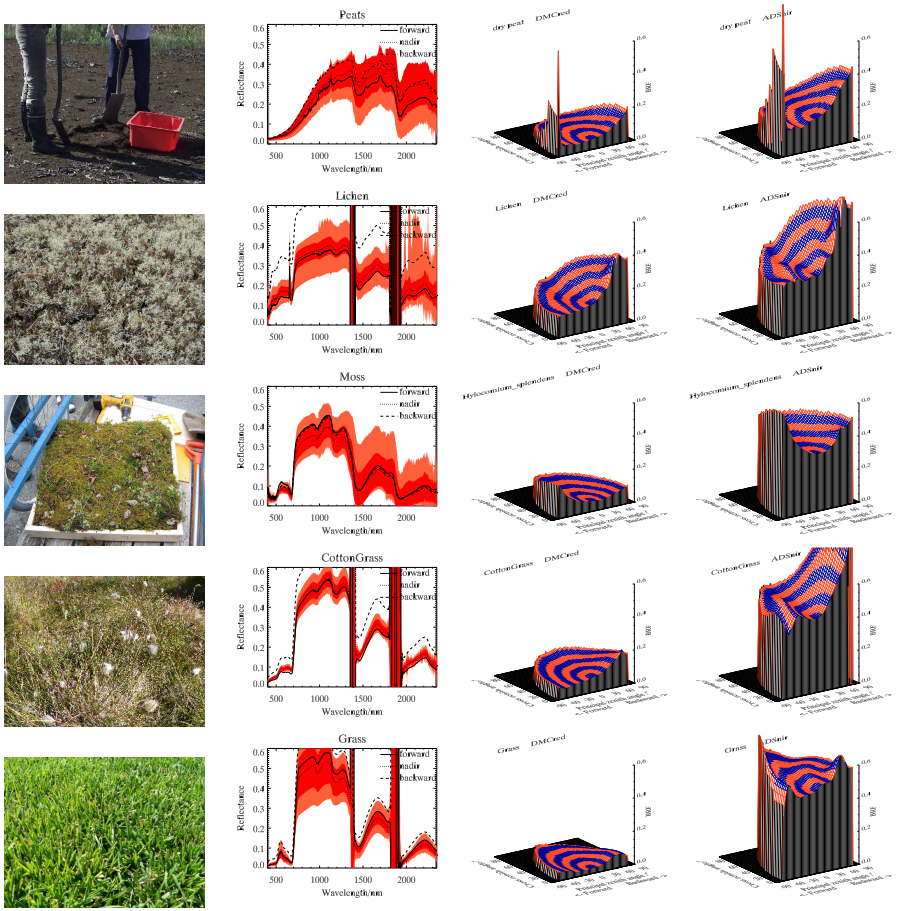

Fig. 4. Continued. Peat, lichen (mostly Cladina arbuscula and C. rangiferina), moss (mostly Hylocomium splendens), cotton grass(angle of incidence: 65°), grass.

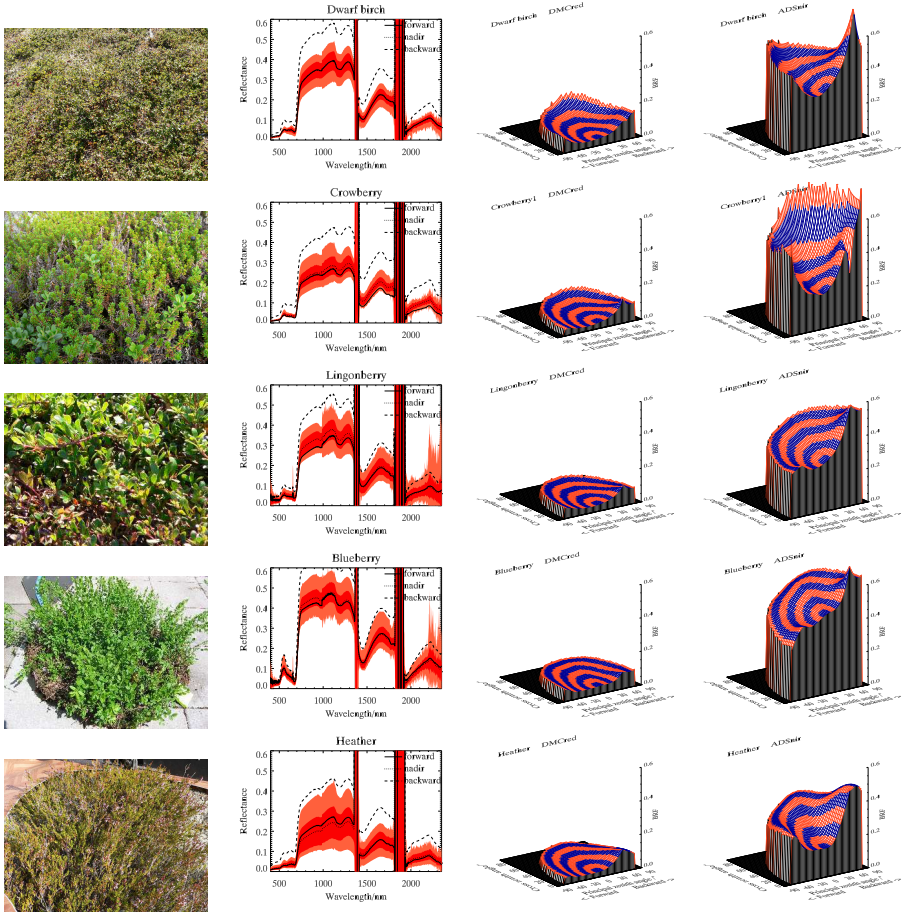

Fig. 4. Continued with dwarf shrubs: dwarf birch, crowberry (angle of incidence: 58°), lingonberry, blueberry, heather.

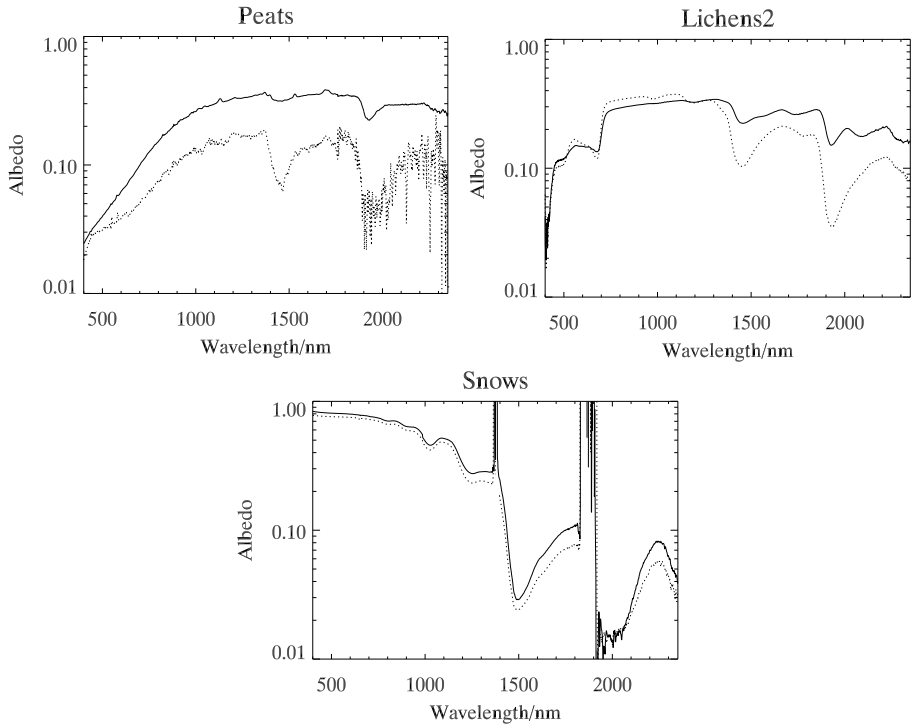

Fig. 5. Spectral albedos of dry (solid line) and wet (dotted line) peat (left), lichen (middle) and snow (right). Wetness effect is very clearly visible in peat, but very faintly in snow, best around 1350–1400 nm (the dominating effect is grain size).

Fig. 6. Typical forest understoreys and openings. Note the strong heterogeneity in all scales, many kinds of vegetation, small scale topography, rocks, small openings, debris from trees.

BGD

5, 1069–1095, 2008